HHS Public Access

Author manuscript

Endocr Relat Cancer. Author manuscript; available in PMC 2020 September 07.

Published in final edited form as:

Endocr Relat Cancer. 2018 October ; 25(10): 853–864. doi:10.1530/ERC-18-0150.

Potent effects of roniciclib alone and with sorafenib against well-differentiated thyroid cancer

Shu-Fu Lin[1,2,*], **Jen-Der Lin**[1,2], **Chuen Hsueh**[2,3], **Ting-Chao Chou**[4,5], **Richard J. Wong**[6]

[1]Department of Internal Medicine, Chang Gung Memorial Hospital, Taoyuan, Taiwan

[2]Chang Gung University, Taoyuan, Taiwan

[3]Department of Pathology, Chang Gung Memorial Hospital, Taoyuan, Taiwan

[4]Laboratory of Preclinical Pharmacology Core, Memorial Sloan-Kettering Cancer Center, New York, NY, USA

[5]Current address: PD Science, Inc., 599 Mill Run, Paramus, NJ, USA

[6]Department of Surgery, Memorial Sloan-Kettering Cancer Center, New York, NY, USA

Abstract

Activation of cyclin-dependent kinase activity is frequently observed in many human cancers; therefore, cyclin-dependent kinases that promote cell cycle transition and cell proliferation may be potential targets in the treatment of malignancy. The therapeutic effects of roniciclib, a cyclin-dependent kinase inhibitor for papillary and follicular thyroid cancer (designated as well-differentiated thyroid cancer), were investigated in this study. Roniciclib inhibited cell proliferation in two papillary and two follicular thyroid cancer cell lines in a dose-dependent manner. Roniciclib activated caspase-3 activity and induced apoptosis. Cell cycle progression was arrested in the G2/M phase. Roniciclib treatment *in vivo* retarded the growth of two well-differentiated thyroid tumors in xenograft models in a dose-dependent fashion. Furthermore, the combination of roniciclib with sorafenib was more effective than either single treatment in a follicular thyroid cancer xenograft model. Acceptable safety profiles appeared in animals treated with either roniciclib alone or roniciclib and sorafenib combination therapy. These findings support roniciclib as a potential drug for the treatment of patients with well-differentiated thyroid cancer.

Keywords

roniciclib; cyclin-dependent kinase; well-differentiated thyroid cancer

[*]**Corresponding author:** Shu-Fu Lin, Department of Internal Medicine, Chang Gung Memorial Hospital, Taoyuan, Taiwan; mmg@cgmh.org.tw; Tel: +886 3 3281200 ext 8821; Fax: +886 3 3288257.

Author contributions

S-FL and RW designed the study; T-CC and RW provided material support; S-FL and CH acquired the data; S-FL, J-DL, T-CC, and RW analyzed and interpreted the data; S-FL wrote the manuscript; and all authors reviewed and revised the manuscript.

Declaration of interest

There is no potential conflict of interest.

Introduction

Thyroid cancer is the most common type of endocrine-related cancer as its incidence has increased in many countries over the past four decades (Kitahara and Sosa, 2016). The main types of thyroid cancer originate from follicular cells (papillary, follicular, Hürthle-cell, poorly differentiated and anaplastic cancer) and parafollicular C cells (medullary cancer) (Fagin and Wells, 2016). More than 85% of patients with thyroid carcinoma have papillary and follicular cancer, known as well-differentiated thyroid cancer (WDTC). Patients with WDTC generally have a favorable prognosis, surviving for more than 10 years following standard treatment with surgery, radioactive iodine (RAI) and thyroid hormone therapy. However, in those patients with metastatic RAI-refractory WDTC, the survival was <3–5 years (Haugen et al., 2016). Two multi-kinase inhibitors, sorafenib and lenvatinib, have been approved for the treatment of metastatic and RAI-refractory WDTC by the U.S. Food and Drug Administration (FDA). However, the therapeutic efficacy of these agents is limited in many patients who develop disease progression, and toxicities have been reported, resulting in dose reduction and termination of treatment (Brose et al., 2014; Schlumberger et al., 2015). Therefore, novel treatments with different therapeutic mechanisms are essential to meet the clinical needs of patients with progressive WDTC.

Uncontrolled cell division is a pathologic manifestation of cancer resulting from aberrant activity of a variety of cell cycle proteins and upstream growth-regulatory signaling that induces cell cycle progression (Otto and Sicinski, 2017). There are four characteristic phases of the cell cycle: gap 1 (G1), DNA synthesis (S), gap 2 (G2), and mitosis (M). Progression of cells through the cell cycle is tightly regulated by multiple cell cycle-associated proteins, including cyclin-dependent kinases (CDKs). Many malignancies are dependent on CDKs for survival and are specifically sensitive to their inhibition (Finn et al., 2009; Otto and Sicinski, 2017). Specific CDKs are activated by complexing with their partner proteins, cyclins. In response to mitogenic signals, the formation of CDK and cyclin complexes, including CDK4/6-cyclin D, CDK2-cyclin E, CDK1/2-cyclin A, and CDK1-cyclin B1 leads to cell cycle entry, cell cycle progression, and cell division (Malumbres and Barbacid, 2009; Asghar et al., 2015; Otto and Sicinski, 2017). In addition to the canonical functions of CDKs, a previous study suggests that mammalian CDKs regulate other cellular process, including cell survival (Hydbring et al., 2016). In addition, CDK5 is pivotal for neuronal survival during development (Cheung et al., 2008). CDK7 is a transcriptional CDK that is required to prevent apoptosis in triple-negative breast cancer cells (Wang et al., 2015). CDK9 is a subunit of the positive transcription elongation factor b complex that is essential for the proliferation and maintenance of oncogenic *MYC*-driven hepatocellular carcinoma (Huang et al., 2014). Given these critical roles for CDKs in cell proliferation and survival, targeting CDKs is considered a potential therapeutic approach for cancer therapy.

Roniciclib is a potent inhibitor of cell cycle CDKs (CDK1, CDK2, CDK3 and CDK4), transcriptional CDKs (CDK5, CDK7 and CDK9) and non-CDK kinases (including Aurora A) with 50% inhibitory concentrations in the low nanomolar range (≤ 25 nmol/L) (Siemeister et al., 2012). Roniciclib inhibits cell cycle transition, promotes caspase-3 activity and stimulates apoptosis *in vitro*. Oral administration of roniciclib has potent efficacy in impeding tumor growth of cervical, lung and anaplastic thyroid cancer xenografts, with

favorable safety profiles in animal models ([a]Lin et al., 2017; Siemeister et al., 2012). The objective of this study was to evaluate the therapeutic effects of roniciclib in WDTC *in vitro* and *in vivo*. Roniciclib induces cytotoxicity in papillary and follicular thyroid cancer cells *in vitro*. Using both papillary and follicular thyroid cancer xenograft models, substantial therapeutic effects and acceptable safety profiles of roniciclib treatment were observed *in vivo*. In addition, the combination of roniciclib and sorafenib, a multikinase inhibitor that suppresses tumor cell proliferation and inhibits angiogenesis (Wilhelm et al., 2006), demonstrated better therapeutic effects than either single agent therapy in WDTC *in vitro* and *in vivo*.

Materials and Methods

Cell lines

Two human papillary thyroid cancer cell lines, BHP7–13 and K1, and two human follicular thyroid cancer cell lines, WRO82–1 and FTC-133, were evaluated. BHP7–13 and WRO82–1 cells were described before ([b]Lin et al., 2017). K1 and FTC-133 were obtained from Sigma (St. Louis, MO, USA). All cell lines were authenticated using DNA (short tandem repeats) profiling and stored in liquid nitrogen until use. These thyroid cancer cell lines are unique cell lines of human thyroid cancer origin harboring various genetic mutations (Schweppe et al., 2008). BHP7–13 and WRO82–1 cells were maintained in RPMI 1640 with sodium bicarbonate (2.0 g/L). K1 cells were maintained in DMEM, Ham's F12 and MCDB 105 (2:1:1) with glutamine (2.0 mmol/L). FTC-133 cells were maintained in DMEM and Ham's F12 (1:1) with glutamine (2.0 mmol/L). All media contained 10% fetal calf serum, 100,000 units/L penicillin and 100 mg/L streptomycin. All cells were maintained in a 5% CO_2 humidified incubator at 37°C.

Pharmacologic agents

Roniciclib and sorafenib were generous gifts from Bayer AG (Berlin, Germany). Roniciclib and sorafenib were dissolved in DMSO (Sigma) to a concentration of 10 mmol/L and stored at −30°C or −80°C until further use for *in vitro* experiments. For the *in vivo* studies, roniciclib was diluted in the vehicle, 40% poly(ethylene glycol) 300 (Sigma) and 60% water to a concentration of 0.357 mg/mL before use. Sorafenib was dissolved in 50% Kolliphor EL (Sigma) and 50% ethanol (Sigma) to a concentration of 57.6 mg/mL and stored at −80°C. Sorafenib was further diluted with water to a final concentration of 14.4 mg/mL before *in vivo* use.

Antibodies

Antibodies targeting cleaved caspase-3, caspase-3, aurora A, cyclin B1 and survivin were purchased from Cell Signaling Technology (Danvers, MA, USA). α-tubulin antibodies were obtained from Sigma.

Cytotoxicity assays and drug efficacy and drug synergy studies

Cells were plated at 2×10^3 to 2×10^4 cells per well in 24-well plates in 1 mL of media. After overnight incubation, six serial two-fold dilutions of roniciclib, sorafenib or vehicle were added over a 4-day treatment course after which cytotoxicity was determined. Culture

medium was removed, and the cells were washed with PBS and lysed with Triton X-100 (1.35%, Sigma) to release intracellular lactate dehydrogenase (LDH), which was quantified with a Cytotox 96 kit (Promega, Madison WI, USA) at 490nm by spectrophotometry (Infinite M200 PRO, Tecan). Each experiment was performed in triplicate, and the results are shown as the percentage of surviving cells determined by comparing the LDH of each sample relative to control samples, which were considered 100% viable. The potency of cytotoxicity of roniciclib in each thyroid cell line was determined by the median-effect plot of the mass-action law using the CompuSyn software (Chou and Martin, 2005; Chou 2006). The median-effect doses (IC50 values) were automatically determined following each set of dose-effect data entries.

For combination therapy studies, cells were treated with roniciclib and sorafenib at a fixed dose ratio. Cells were incubated with vehicle, roniciclib, sorafenib or combination therapy simultaneously for a 4-day course after which cytotoxicity was measured. Six serial two-fold dilutions were examined at the following starting doses for BHP7–13, K1, WRO82–1 and FTC-133: roniciclib at 75.2, 66.8, 30.8 and 76.0 nmol/L and sorafenib at 2.8, 18.0, 4.0 and 23.6 mmol/L. The doses were chosen based on the determined IC50. Interactions between roniciclib and sorafenib *in vitro* were assessed by calculating the combination index (CI) using the Chou-Talalay equation and CompuSyn software (Chou and Martin, 2005; Chou 2006). Synergy (CI < 1), additive effect (CI = 1) and antagonism (CI > 1) are quantitatively determined by CompuSyn simulation at different effect levels.

Apoptosis assessment

Caspase-3 activity was analyzed using a fluorometric assay kit (Abcam, Cambridge, MA, USA). Cells were plated at 1×10^6 cells in 100-mm Petri dishes in 10 mL of media overnight. Roniciclib (25 nmol/L) or vehicle was added for 24 h. Adherent cells (5×10^5) were collected, centrifuged and lysed using 50 μL of lysis buffer on ice for 10 min, and incubated with DEVD-AFC substrate and reaction buffer at 37°C for 1.5 h. Caspase-3 activity was detected by spectrophotometry. Each condition was performed in duplicate.

The ability of roniciclib to induce sub-G1 apoptotic cell accumulation was studied using flow cytometry. Cells were plated at 2×10^5 cells (BHP7–13 and WRO82–1) and 4×10^5 cells (K1 and FTC-133) per well in 6-well plates in 2 mL media overnight. Roniciclib (25 nmol/L) or vehicle was added and incubated for 24 h. Floating cells and trypsinized adherent cells were collected, washed with PBS, fixed with cold 70% ethanol and incubated with RNase A (100 μg/mL; Sigma) and propidium iodide (5 μg/mL; Sigma) at 37°C for 15 min. Apoptotic sub-G1 cells were identified by DNA content analysis of 1×10^4 events for each sample by flow cytometry (BD FACScalibur Flow Cytometer, BD Biosciences, Billerica, MA, USA). Each condition was performed in triplicate.

Cell cycle assessment

The effects of roniciclib on cell cycle progression were evaluated. Cells were plated at 3×10^5 (WRO82–1) and 4×10^5 cells (BHP7–13, K1 and FTC-133) per well in 6-well plates in 2 mL of media overnight. Roniciclib (25 nmol/L) or vehicle was added and incubated for 24 h, after which adherent cells were collected, and samples were prepared as described above

for sub-G1 apoptosis. Cell cycle distribution was identified by DNA content analysis of 1×10^4 events for each sample by flow cytometry (BD FACScalibur Flow Cytometer, BD Biosciences). Each condition was performed in triplicate.

Immunofluorescence microscopy

The expression of cleaved caspase-3 was evaluated using immunofluorescence microscopy. Thyroid cancer cells were plated at 1×10^5 cells in 4-well culture slides in 1 mL of media overnight. Cells were treated with roniciclib (25 nmol/L) or placebo for 24 h, washed with PBS, fixed in 4% paraformaldehyde (Sigma) for 15 min at room temperature, washed with PBS, permeabilized with 0.1% Triton X-100 (10 min, room temperature) and washed with PBS. Cells were then incubated with primary rabbit cleaved caspase-3 antibody (1:400) and mouse α-tubulin antibody (1:1000) at 4°C overnight, washed with PBS and incubated with secondary Alexa Fluor 633-conjugated goat anti-rabbit antibody (1:1000; Invitrogen, Carlsbad, CA, USA) and Alexa Fluor 488-conjugated goat anti-mouse antibody (1:1000; Life Technologies, Coraopolis, PA, USA) for 25 min at 37°C, washed with PBS, incubated with 4′,6-diamidino-2-phenylindole (DAPI; 0.2 μg/mL, Invitrogen) for 10 min at room temperature, washed with PBS and covered with mounting medium. Images were acquired using Leica TCS SP8 X confocal microscopy (Leica Microsystems).

The effect of roniciclib on mitosis was evaluated using confocal microscopy. Thyroid cancer cells were plated at 1×10^5 cells in 4-well culture slides in 1 mL of media overnight. Roniciclib (25 nmol/L) or placebo-treated thyroid cancer cell samples were prepared as described above. Cells were then incubated with the primary mouse α-tubulin antibody (1:1000) at 4°C overnight, washed with PBS, incubated with secondary Alexa Fluor 488-conjugated goat anti-mouse antibody (1:1000; Life Technologies) for 25 min at 37°C, washed with PBS, counterstained with DAPI, washed with PBS and covered with Vectashield mounting medium (Vector Laboratories, Burlingame, CA, USA). Images were captured with Leica TCS SP8 X confocal microscopy (Leica Microsystems). Chromosomes were examined to identify mitotic cells.

Western blot analysis

Thyroid cancer cells were plated at 1×10^6 cells in 100-mm Petri dishes in 10 mL of media overnight and treated with roniciclib at 25 nmol/L or vehicle for the indicated periods. Cell pellets were dissolved in radio-immunoprecipitation assay buffer and protease inhibitor cocktail, vortexed and clarified by centrifugation. Total protein (20–40 μg) was separated by electrophoresis on 12% Tris-HCl gels, transferred to polyvinylidene difluoride membranes, blocked and exposed to primary antibodies followed by a secondary antibody conjugated to horseradish peroxidase. Signals were developed using an enhanced chemiluminescence kit (PerkinElmer, Waltham, MA, USA). Band density was imaged and quantified using Molecular Imager VersaDoc MP 4000 system (Bio-Rad). The ratios of each protein to α-tubulin were calculated.

Flank xenograft tumor therapy

Female athymic nude mice 8–10 weeks of age from the National Laboratory Animal Center, Taiwan, were anesthetized with an intraperitoneal injection of 2% 2,2,2-tribromoethanol

(200 μL/mouse; Sigma) before implantation of thyroid cancer cells. K1 and FTC-133 flank tumors were established by injecting 1×10^6 cells in 100 μL of extracellular matrix (ECM) gel (Sigma) into the subcutaneous flanks of nude mice. K1 and FTC-133 cell lines were chosen in this study because they had high tumorigenesis rates in murine models. Treatment started 22 days after K1 cells implantation and 28–29 days after FTC-133 cells implantation.

For monotherapy with roniciclib, mice bearing K1 and FTC-133 xenograft tumors received oral administration of vehicle or roniciclib (1.0 mg/kg and 1.3 mg/kg) twice a day for two cycles of 4-day on and 3-day off therapy (Siemeister et al., 2012). For roniciclib and sorafenib combination therapy, mice bearing thyroid tumors received placebo, roniciclib (1.4 mg/kg), sorafenib (25 mg/kg) or simultaneous combination treatment once a day for three cycles of 4-day on and 3-day off treatment. Tumor dimensions were serially measured with electronic calipers, and the volumes were calculated by the following formula: $a \times b^2 \times 0.4$, where a represents the largest diameter and b is the perpendicular diameter. The body weight of each animal was followed as a marker of toxicity. Relative tumor growth of each xenograft was calculated as $Vx/V1$, where Vx is the volume in mm^3 at an indicated time and $V1$ at the beginning of treatment.

Tumor levels of cleaved caspase-3, aurora A, cyclin B1 and survivin were evaluated in mice treated with oral dosing of roniciclib (1.3 mg/kg) by Western blot analysis. At indicated periods, animals were euthanized with carbon dioxide, and the tumors were harvested and snap freezing in liquid nitrogen before sample preparation, followed by mixed with protein extraction buffer (GE Healthcare), homogenized and sonicated on ice. After centrifugation, clarified supernatants were aliquoted and stored at −80°C until Western blot analyses.

This study was approved by the Committee of Laboratory Animal Center at the Chang Gung Memorial Hospital, Linkou (permission No: 2013121401) and performed in accordance with the recommendations in the Guide for the Care and Use of Laboratory Animals of the Chang Gung Memorial Hospital.

Statistical analyses

Comparisons were performed when appropriate, using two-sided Student's *t* tests (Excel, Microsoft). Results are expressed as mean ± SE. $P<0.05$ was considered statistically significant.

Results

Cytotoxicity of roniciclib in WDTC cell lines

Roniciclib inhibited cell survival in two papillary thyroid cancer cell lines (BHP7–13 and K1 cells) and two follicular thyroid cancer cell lines (WRO82–1 and FTC-133 cells) in a dose-dependent manner (Fig. 1). Roniciclib at 25 nmol/L inhibited cell growth by 74.4% (BHP7–13), 80.4% (K1), 63.6% (WRO82–1) and 70.9% (FTC-133) at day 4. At 100 nmol/L, roniciclib arrested cell growth by 93.2% (BHP7–13), 98.5% (K1), 74.2% (WRO82–1) and 96.1% (FTC-133) at day 4. The cytotoxicity potency of roniciclib in WDTC cancer cell lines was determined using CompuSyn software. The median-effect dose (IC50) was determined on day 4. In papillary thyroid cancer cell lines, K1 cells had a lower IC50 (16.7 ± 0.1

nmol/L) than that of BHP7–13 cells (18.8 ± 0.6 nmol/L). In follicular thyroid cancer cell lines, WRO82–1 cells had a lower IC50 (9.8 ± 2.8 nmol/L) than that of FTC-133 cells (19.0 ± 0.1 nmol/L).

Roniciclib induced apoptosis in WDTC cell lines

Apoptosis has an important role in cancer therapy (Galluzzi et al., 2012). Roniciclib activates caspase-3 activity and induces apoptosis in HeLa and anaplastic thyroid cancer cell lines (Siemeister et al., 2012; [a]Lin et al., 2017). Therefore, we evaluated the effects of roniciclib on apoptosis in papillary and follicular thyroid cancer cell lines. The effects of roniciclib (25 nmol/L) on caspase-3 activity in BHP7–13, K1, WRO82–1 and FTC-133 cell lines were determined using a fluorometric assay at 24 h (Fig. 2A). Roniciclib significantly increased caspase-3 activity compared to control treatment in BHP7–13, K1, WRO82–1 and FTC-133 cells, demonstrating activation of caspase-3. Caspase-3 activation was also assessed by detection of cleaved caspase-3 using immunofluorescent analysis in papillary and follicular thyroid cancer cell lines. A representative cell line, BHP7–13 cells, was shown (Fig. 2B). The percentages of cells with cleaved caspase-3 expression were analyzed (Fig. 2C). Roniciclib (25 nmol/L for 24 h) significantly increased the proportions of cells with cleaved caspase-3 expression in BHP7–13, K1, WRO82–1 and FTC-133 cell lines when compared with the corresponding controls. Thus, activation of caspase-3 may lead to apoptotic cell death.

The ability of roniciclib to induce sub-G1 apoptosis in papillary and follicular thyroid cancer cell lines was evaluated. A representative cell line, BHP7–13 cells, was shown (Supplementary Fig. 1). BHP7–13, K1, WRO82–1 and FTC-133 cell lines were exposed to roniciclib (25 nmol/L for 24 h), and the proportion of sub-G1 apoptotic cells was calculated (Fig. 2D). Roniciclib significantly induced higher proportions of sub-G1 cells in BHP7–13 cells, K1, WRO82–1 and FTC-133 cells as compared to the control treatment. These data indicate that roniciclib induces apoptosis in papillary and follicular thyroid cancer cells.

Effects of roniciclib on the cell cycle

The effect of roniciclib (25 nmol/L for 24 h) on cell cycle distribution in papillary and follicular thyroid cancer cell lines was evaluated. A representative cell line, BHP7–13 cells, was shown (Fig. 3A), and the cell cycle data was analyzed (Fig. 3B). Compared with placebo treatment, roniciclib significantly induced cell accumulation in the G2/M phase in BHP7–13, K1, WRO82–1 and FTC-133 cells, demonstrating induction of G2/M arrest.

The ability of roniciclib to arrest cells in the mitotic phase was determined using a confocal microscopy. A representative cell line, BHP7–13 cells, was shown (Supplementary Fig. 2). Mitotic cells were identified, and the mitotic index was calculated for papillary and follicular thyroid cancer cell lines (Fig. 3C). Compared with the control treatment, roniciclib (25 nmol/L) treatment for 24 h significantly decreased the percentage of mitotic cells in BHP7–13, K1, WRO82–1 and FTC-133 cell lines, demonstrating that roniciclib prevented thyroid cancer cells progression into mitosis.

Roniciclib modulates the expression of aurora A and cyclin B1

Aurora A and cyclin B1 are essential for G2/M transition and mitotic progression (Marumoto et al., 2002; Lindqvist et al., 2007; Cowley et al., 2009). Inhibition of aurora A and cyclin B1 results in cell accumulation in G2/M phase. The effects of roniciclib (25 nmol/L) on the expression of these proteins were evaluated in papillary and follicular thyroid cancer cell lines (Fig. 3D). Aurora A levels decreased by 8 h, with inhibitory effects persisting for 24 h in BHP7–13, K1, WRO82–1 and FTC-133 cell lines. In BHP7–13 and K1 cells, cyclin B1 levels decreased by 8 h, and the inhibitory effects persisted for 24 h. In WRO82–1 cells, cyclin B1 levels transiently increased by 4 h, then decreased by 16 h with inhibitory effects persisting for 24 h. In the FTC-133 cell line, cyclin B1 expression increased at 16 h, followed by decreasing at 24 h. These results demonstrate that 24-h roniciclib treatment diminishes aurora A and cyclin B1 expression in BHP7–13, K1, WRO82–1 and FTC-133 cells.

Monotherapy with roniciclib for murine flank WDTC tumors

Female nude mice bearing flank xenografts of K1 cells were used to evaluate the therapeutic efficacy and safety of roniciclib in papillary thyroid cancer *in vivo*. Animals with established K1 flank tumors with a mean diameter of 4.0 mm were treated with oral gavage of placebo ($n = 6$), low-dose roniciclib (1.0 mg/kg, $n = 6$) or high-dose roniciclib (1.3 mg/kg, $n = 6$) twice a day for two cycles of a 4-day on and 3-day off therapy. Low-dose roniciclib treatment significantly retarded K1 tumor growth by day 3 as compared to the control group (1.2 ± 0.1-fold and 1.6 ± 0.1-fold, $P = 0.047$), and the effect persisted through day 14 (1.5 ± 0.3-fold and 17.6 ± 3.0-fold, $P < 0.001$; Fig. 4A). High-dose roniciclib treatment also significantly retarded K1 tumor growth by day 3 (1.1 ± 0.1-fold and 1.6 ± 0.1-fold, $P = 0.005$), and the effect persisted until day 14 (0.7 ± 0.1-fold and 17.6 ± 3.0-fold, $P < 0.001$). Of note, high-dose roniciclib treatment caused tumor regression in all six mice by day 14, and this tumor-regression effect persisted in two mice until day 27. Serial administration of low- and high-dose roniciclib did not result in statistically significant body weight change during the study period (Fig. 4B). However, high-dose roniciclib treatment induced a 12% weight loss in one mouse on day 3, which was managed with immediate discontinuation of treatment. This weight loss recovered before the second cycle of treatment and thereafter.

The therapeutic efficacy and safety of roniciclib in follicular thyroid cancer *in vivo* were evaluated in female nude mice bearing flank xenografts of FTC-133. Animals with established FTC-133 flank tumors with a mean diameter of 4.8 mm were treated with oral gavage of placebo ($n = 6$), low-dose roniciclib (1.0 mg/kg, $n = 6$) and high-dose roniciclib (1.3 mg/kg, $n = 6$) twice a day for two cycles of a 4-day on and 3-day off therapy. Low-dose roniciclib treatment significantly retarded FTC-133 tumor growth by day 3 as compared to the control group (1.1 ± 0.1-fold and 1.9 ± 0.2-fold, $P = 0.001$), and the effect persisted through day 21 (4.5 ± 0.8-fold and 19.4 ± 2.3-fold, $P < 0.001$; Fig. 4C). High-dose roniciclib treatment also significantly retarded FTC-133 tumor growth by day 3 (1.1 ± 0.0-fold and 1.9 ± 0.2-fold, $P < 0.001$), and the effect persisted until day 21 (4.4 ± 0.8-fold and 19.4 ± 2.3-fold, $P < 0.001$). Serial treatment of high-dose roniciclib slightly and significantly induced body weight loss on day 10 when compared with control mice bearing FTC-133 xenografts

(Fig. 4D). Representative mice bearing K1 (Fig. 4E) and FTC-133 (Fig. 4F) tumors were photographed after a 15-day treatment.

The molecular effects of high-dose roniciclib (1.3 mg/kg) treatment in K1 xenografts were evaluated using Western blot analysis (Fig. 4G). The ratios of cleaved caspase-3, aurora A and cyclin B1 to α-tubulin were calculated. Relative expression was calculated using baseline values as a reference (Supplementary Fig. 3A). Roniciclib treatment rapidly (by 2 h) increased the levels of cleaved caspase-3. Aurora A level was transiently increased between 2 h and 4 h, then decreased by 10 h with inhibitory effect persisted till 24 h. Cyclin B1 level was transiently increased between 2 h and 4 h, then decreased by 8 h. The molecular effects of high-dose roniciclib (1.3 mg/kg) treatment in FTC-133 xenografts were also evaluated using immunoblot analysis (Fig. 4H). Roniciclib treatment increased cleaved caspase-3 expression at 4 h, and this effect was greater at 24 h. Aurora A levels were decreased between 2 h and 8 h, increasing at 10 h and then decreasing at 24 h. Cyclin B1 level was transiently increased between 2 h and 8 h, decreasing at 10 h and then increasing at 24 h.

Interaction of roniciclib and sorafenib in WDTC cells

Sorafenib has demonstrated efficacy in the treatment of patients with WDTC (Brose et al., 2014). However, some patients are refractory to sorafenib treatment, and strategies to improve its therapeutic efficacy are required. Thus, we evaluated the interactions between roniciclib and sorafenib in papillary and follicular thyroid cancer cell lines.

The cytotoxic effects of sorafenib in BHP7–13, K1, WRO82–1 and FTC-133 cells were analyzed (Fig. 5A), showing that sorafenib inhibited cell proliferation in a dose-dependent manner. At 1.25 μmol/L, sorafenib inhibited cell growth by 62.8% (BHP7–13), 2.5% (K1), 62.9% (WRO82–1) and 10.4% (FTC-133) by day 4. At 10 μmol/L, sorafenib arrested cell growth by >91% in BHP7–13, K1, WRO82–1 and FTC-133 cells. The IC50 of sorafenib on day 4 for each cell line is shown in Fig. 5B.

Interactions between roniciclib and sorafenib were evaluated in papillary and follicular thyroid cancer cell lines (Fig. 5C). In WRO82–1 cells, the combination of roniciclib and sorafenib had remarkedly improved cytotoxicity over single agent therapies across all doses of treatment. In addition, roniciclib and sorafenib combination therapy significantly improved cytotoxicity over single agent therapies at lower doses of treatment in BHP7–13, K1 and FTC-133 cells. The CI of roniciclib and sorafenib was analyzed using the Chou-Talalay method, which showed that the combination of roniciclib and sorafenib ranged from synergistic to additive in BHP7–13 cells (CI; 0.68–1.00), synergistic to antagonist in K1 cells (CI; 0.73–1.16) and synergistic in WRO82–1 and FTC-133 cells (CI; 0.54–0.56 and 0.79–0.99, respectively; Fig. 5D). These data revealed that combination therapy of roniciclib and sorafenib were primarily synergistic in BHP7–13, K1, WRO82–1 and FTC-133 cell lines.

Combination therapy of roniciclib and sorafenib for murine flank thyroid tumors

We sought to evaluate the effect of roniciclib and sorafenib combination therapy in mice bearing K1 and FTC-133 xenografts. In a pilot study to evaluate the therapeutic effects of

daily roniciclib therapy (1.4 mg/kg) in K1 tumors with a mean diameter of 4.9 mm (n = 5 – 6 per group), daily roniciclib treatment for 4 doses was sufficient to inhibit K1 tumor growth compared with control treatment on day 7 (1.1 ± 0.2-fold and 3.4 ± 0.5-fold, P = 0.005; Fig. 6A). Daily treatment of roniciclib did not induce significant changes in body weight (Fig. 6B). This potent efficacy of roniciclib single therapy precluded the analysis of roniciclib and sorafenib combination therapy in the treatment of K1 xenografts. Animals with established FTC-133 flank tumors with a mean diameter of 6.5 mm were treated with oral gavage of placebo (n = 6), roniciclib (1.4 mg/kg, n = 5), sorafenib (25 mg/kg, n = 5) or combination therapy (n = 5) once a day for three cycles of 4-day on and 3-day off therapy (Fig. 6C). This dose of sorafenib was lower than that used in a previous study (30–80 mg/kg; Kim et al., 2007). Compared with control treatment, roniciclib, sorafenib and combination therapy all significantly retarded FTC-133 tumor growth by day 3 (1.7 ± 0.1-fold, 1.2 ± 0.1-fold, 1.2 ± 0.1-fold and 1.1 ± 0.1-fold, respectively), and the inhibitory effects persisted in all groups through day 13 (4.6 ± 0.3-fold, 2.9 ± 0.3-fold, 3.4 ± 0.2-fold and 2.2 ± 0.3-fold, respectively). Combination therapy significantly retarded FTC-133 tumor growth on day 17 compared with the roniciclib group (2.7 ± 0.5-fold and 4.4 ± 0.4-fold, P = 0.027) and the sorafenib group (2.7 ± 0.5-fold and 5.2 ± 0.1-fold, P = 0.001). This inhibitory effect of combination therapy persisted through day 20. Serial treatment of placebo, roniciclib, sorafenib or combination therapy did not result in significant changes in body weight as compared with baseline values (Fig. 6D).

Discussion

Roniciclib effectively inhibited cell survival with a relatively low median-effect dose (≤ 19.0 nmol/L) in papillary and follicular thyroid cancer cell lines. Roniciclib treatment alone and in combination of sorafenib effectively prohibited tumor growth of well-differentiated thyroid cancer xenograft models with favorable safety profiles, indicating that this drug has the potential for clinical evaluations in the treatment of patients with WDTC.

Tumor cells often escape apoptosis and induction of apoptosis is considered an important mechanism of anti-cancer therapies. Many CDKs are involved in the apoptosis signaling pathways (Hydbring et al., 2016); therefore, inhibition of CDK activity is likely to contribute to the apoptotic response. Roniciclib treatment activated caspase-3 activity and caused apoptosis in WDTC cell lines, which is likely one of the mechanisms of cytotoxicity in the treatment of thyroid cancer. However, the underlying mechanisms of roniciclib in inducing apoptosis of WDTC cells are not clear and need to be explored in further studies.

Roniciclib arrested BHP7–13, K1, WRO82–1 and FTC-133 cells in the G2/M phase; it also decreased the proportions of cells in the mitotic phase. Therefore, G2 phase arrest is likely one of the mechanisms of cytotoxicity in WDTC cell lines, which may be mediated by decreased levels of aurora A and cyclin B1. Aurora A is a serine/threonine kinase that is required for G2 to M transition and mitotic progression (Marumoto et al., 2002; Cowley et al., 2009). Cyclin B1 is essential to activate CDK1 activity in the late G2 phase, a key event for mitotic entry (Lindqvist et al., 2007). During mitosis, increasing CDK1-cyclin B1 activity is required for mitotic progression from prophase to prometaphase and metaphase. The effects of decreased levels of aurora A and cyclin B1 may range from a failure in the

G2/M transition to mitotic arrest. In this study, roniciclib accumulated cells in the G2 phase in all four WDTC cell lines.

Roniciclib treatment also significantly repressed K1 and FTC-133 tumor growth. The anti-tumor effects are likely mediated through both apoptosis induction and cell cycle inhibition given that cleaved caspase-3 levels increased and aurora A and cyclin B1 levels decreased with roniciclib treatment. In K1 and FTC-133 tumors, increased cleaved caspase-3 levels appeared just 2–4 h following roniciclib administration, indicating that this effects was rapid. Roniciclib therapy led to stronger inhibitory effects on the expression of aurora A and cyclin B1 in K1 tumors as compared with that in FTC-133 tumors. These robust effects may later lead to better tumor volume inhibition in K1 tumors. However, roniciclib treatment *in vivo* transiently increased aurora A and cyclin B1 levels before decreasing them in K1 and FTC-133 xenografts. Thus, strategies to inhibit aurora A and cyclin B1 may enhance the therapeutic effects of roniciclib in the treatment of WDTC tumors.

Sorafenib therapy is approved by the U.S. FDA in the treatment of WDTC. However, some patients with refractory WDTC discontinued sorafenib treatment because of drug intolerance or treatment failures (Brose et al., 2014). Strategies to improve the therapeutic effects of sorafenib are needed. In this study, we found favorable effects following roniciclib and sorafenib combination therapy in the treatment of FTC-133 tumors. This combination therapy inhibited FTC-133 tumor growth significantly better than either drug treatment alone with promising safety profiles. The promising effects of combination therapy *in vivo* may be through action mechanisms of these drugs, including arrest of cell cycle, induction of apoptosis and inhibition of angiogenesis.

Survivin is an inhibitor of proteins involved in apoptosis inhibition and regulation of the cell cycle (Vong et al., 2005; Rosa et al., 2006; Carmena et al., 2012). Our previous data has revealed that roniciclib decreased survivin expression in anaplastic thyroid cancer ([a]Lin et al., 2017). Thus, we evaluated the effects of roniciclib on the expression of survivin in WDTC *in vitro* and *in vivo*. Survivin levels were decreased after roniciclib treatment in four WDTC cell lines and two WDTC xenograft models (Supplementary Fig. 4).

A recent phase I clinical trial shows roniciclib reached a Cmax of 98.6 μg/L (Bahleda et al., 2017). This corresponds to a total Cmax of 229 nmol/L. Upon correction for plasma protein binding, the free concentration of roniciclib reached in the clinical setting was about 14 nmol/L. The ≤ 19 nmol/L median-effect dose provided in this study corresponds to a free concentration of roniciclib of ≤ 15.8 nmol/L upon correction for culture media protein binding. These calculations support that the roniciclib concentrations are close to the free concentrations of roniciclib which had been achieved in phase I studies.

Our present and prior studies demonstrate roniciclib was an effective treatment for both well-differentiated and undifferentiated thyroid cancer, revealing the broad therapeutic activity of roniciclib for a variety of thyroid cancer with different genetic alterations, and regardless of the ability of iodine uptake (Feng et al., 2011; [a]Lin et al., 2017). Our findings encourage future clinical trials using roniciclib for the treatment of patients with refractory thyroid cancer.

Conclusions

Roniciclib induces cytotoxicity in both papillary and follicular thyroid cancer cell lines. Using K1 and FTC-133 xenograft tumors, the therapeutic efficacy and safety of roniciclib treatment were demonstrated. Roniciclib and sorafenib combination therapy exhibited greater therapeutic efficacy over either single treatment in FTC-133 tumors. These data support the clinical evaluation of roniciclib in the treatment of patients with WDTC.

Supplementary Material

Refer to Web version on PubMed Central for supplementary material.

Acknowledgements

We acknowledge Bayer AG (Berlin, Germany) for providing roniciclib and sorafenib. We thank the staff of the Microscope Core Laboratory, the Laboratory Animal Center, and the Expensive Advanced Instrument Core Laboratory of the Chang Gung Memorial Hospital at Linkou for technical support.

Funding

This work was supported by the Chang Gung Memorial Hospital (grant no. CMRPG3H0201 and CMRPG3E0353) and the Ministry of Science and Technology of Taiwan (grant no. MOST 106-2314-B-182A-095).

References

Asghar U, Witkiewicz AK, Turner NC & Knudsen ES 2015 The history and future of targeting cyclin-dependent kinases in cancer therapy. Nature Reviews Drug Discovery 14 130–146. [PubMed: 25633797]

Bahleda R, Grilley-Olson JE, Govindan R, Barlesi F, Greillier L, Perol M, Ray-Coquard I, Strumberg D, Schultheis B, Dy GK et al. 2017 Phase I dose-escalation studies of roniciclib, a pan-cyclin-dependent kinase inhibitor, in advanced malignancies. British Journal of Cancer 116 1505–1512. [PubMed: 28463960]

Brose MS, Nutting CM, Jarzab B, Elisei R, Siena S, Bastholt L, de la Fouchardiere C, Pacini F, Paschke R, Shong YK et al. 2014 Sorafenib in radioactive iodine-refractory, locally advanced or metastatic differentiated thyroid cancer: a randomised, double-blind, phase 3 trial. Lancet 384 319–328. [PubMed: 24768112]

Carmena M, Wheelock M, Funabiki H & Earnshaw WC 2012 The chromosomal passenger complex (CPC): from easy rider to the godfather of mitosis. Nature Review Molecular Cellular Biology 13 789–803. [PubMed: 23175282]

Cheung ZH, Gong K & Ip NY 2008 Cyclin-dependent kinase 5 supports neuronal survival through phosphorylation of Bcl-2. Journal of Neuroscience 28 4872–4877. [PubMed: 18463240]

Chou TC 2006 Theoretical basis, experimental design, and computerized simulation of synergism and antagonism in drug combination studies. Pharmacology Review 58 621–681.

Chou TC & Martin N 2005 CompuSyn for Drug Combinations: PC Software and Users Guide: A Computer Program for Quantitation of Synergism and Antagonism in Drug Combinations and the Determination of IC50, ED50, and LD50 Values. ComboSyn Available at: www.combosyn.com.

Cowley DO, Rivera-Pérez JA, Schliekelman M, He YJ, Oliver TG, Lu L, Lu L, O'Quinn R, Salmon ED, Magnuson T et al. 2009 Aurora-A kinase is essential for bipolar spindle formation and early development. Molecular and Cellular Biology 29 1059–1071. [PubMed: 19075002]

Fagin JA & Wells SA Jr 2016 Biologic and Clinical Perspectives on Thyroid Cancer. New England Journal of Medicine 375 1054–1067. [PubMed: 27626519]

Feng F, Wang H, Fu H, Wu S, Ye Z, Chen S & Li J 2011 Dedifferentiation of differentiated thyroid carcinoma cell line FTC-133 is enhanced by 131I pretreatment. Nuclear medicine and biology 38 1053–1058. [PubMed: 21982575]

Finn RS, Dering J, Conklin D, Kalous O, Cohen DJ, Desai AJ, Ginther C, Atefi M, Chen I, Fowst C et al. 2009 PD 0332991, a selective cyclin D kinase 4/6 inhibitor, preferentially inhibits proliferation of luminal estrogen receptor-positive human breast cancer cell lines in vitro. Breast Cancer Research 11 R77. [PubMed: 19874578]

Galluzzi L, Vitale I, Abrams JM, Alnemri ES, Baehrecke EH, Blagosklonny MV, Dawson TM, Dawson VL, El-Deiry WS, Fulda S et al. 2012 Molecular definitions of cell death subroutines: recommendations of the Nomenclature Committee on Cell Death 2012. Cell Death and Differentiation 19 107–120. [PubMed: 21760595]

Haugen BR, Alexander EK, Bible KC, Doherty GM, Mandel SJ, Nikiforov YE, Pacini F, Randolph GW, Sawka AM, Schlumberger M et al. 2016 2015 American Thyroid Association Management Guidelines for Adult Patients with Thyroid Nodules and Differentiated Thyroid Cancer: The American Thyroid Association Guidelines Task Force on Thyroid Nodules and Differentiated Thyroid Cancer. Thyroid 26 1–133. [PubMed: 26462967]

Huang CH, Lujambio A, Zuber J, Tschaharganeh DF, Doran MG, Evans MJ, Kitzing T, Zhu N, de Stanchina E, Sawyers CL et al. 2014 CDK9-mediated transcription elongation is required for MYC addiction in hepatocellular carcinoma. Genes and Development 28 1800–1814. [PubMed: 25128497]

Hydbring P, Malumbres M & Sicinski P 2016 Non-canonical functions of cell cycle cyclins and cyclin-dependent kinases. Nature Reviews Molecular Cellular Biology 17 280–292. [PubMed: 27033256]

Kim S, Yazici YD, Calzada G, Wang ZY, Younes MN, Jasser SA, El-Naggar AK & Myers JN 2007 Sorafenib inhibits the angiogenesis and growth of orthotopic anaplastic thyroid carcinoma xenografts in nude mice. Molecular Cancer Therapy 6 1785–1792.

Kitahara CM & Sosa JA 2016 The changing incidence of thyroid cancer. Nature Reviews Endocrinology 12 646–653.

Lin SF, Lin JD, Hsueh C, Chou TC & Wong RJ 2017 Effects of roniciclib in preclinical models of anaplastic thyroid cancer. Oncotarget 8 67990–8000. [PubMed: 28978090]

Lin SF, Lin JD, Hsueh C, Chou TC & Wong RJ 2017 A cyclin-dependent kinase inhibitor, dinaciclib in preclinical treatment models of thyroid cancer. PLoS One 12 e0172315. [PubMed: 28207834]

Lindqvist A, van Zon W, Karlsson Rosenthal C & Wolthuis RM 2007 Cyclin B1-Cdk1 activation continues after centrosome separation to control mitotic progression. PLoS Biology 5 e123. [PubMed: 17472438]

Malumbres M & Barbacid M 2009 Cell cycle, CDKs and cancer: a changing paradigm. Nature Reviews Cancer 9 153–166. [PubMed: 19238148]

Marumoto T, Hirota T, Morisaki T, Kunitoku N, Zhang D, Ichikawa Y, Sasayama T, Kuninaka S, Mimori T, Tamaki N et al. 2002 Roles of aurora-A kinase in mitotic entry and G2 checkpoint in mammalian cells. Genes Cells 7 1173–1182. [PubMed: 12390251]

Otto T & Sicinski P 2017 Cell cycle proteins as promising targets in cancer therapy. Nature Reviews Cancer 17 93–115. [PubMed: 28127048]

Rosa J, Canovas P, Islam A, Altieri DC & Doxsey SJ 2006 Survivin modulates microtubule dynamics and nucleation throughout the cell cycle. Molecular Biology of the Cell 17 1483–1493. [PubMed: 16407408]

Schlumberger M, Tahara M, Wirth LJ, Robinson B, Brose MS, Elisei R, Habra MA, Newbold K, Shah MH, Hoff AO et al. 2015 Lenvatinib versus placebo in radioiodine-refractory thyroid cancer. New England Journal of Medicine 372 621–630. [PubMed: 25671254]

Schweppe RE, Klopper JP, Korch C, Pugazhenthi U, Benezra M, Knauf JA, Fagin JA, Marlow LA, Copland JA, Smallridge RC et al. 2008 Deoxyribonucleic acid profiling analysis of 40 human thyroid cancer cell lines reveals cross-contamination resulting in cell line redundancy and misidentification. Journal of Clinical Endocrinology & Metabolism 93 4331–4341. [PubMed: 18713817]

Siemeister G, Lücking U, Wengner AM, Lienau P, Steinke W, Schatz C, Mumberg D & Ziegelbauer K 2012 BAY 1000394, a novel cyclin-dependent kinase inhibitor, with potent antitumor activity in mono- and in combination treatment upon oral application. Molecular Cancer Therapy 11 2265–2273.

Vong QP, Cao K, Li HY, Iglesias PA & Zheng Y 2005 Chromosome alignment and segregation regulated by ubiquitination of survivin. Science 310 1499–1504. [PubMed: 16322459]

Wang Y, Zhang T, Kwiatkowski N, Abraham BJ, Lee TI, Xie S, Yuzugullu H, Von T, Li H, Lin Z et al. 2015 CDK7-dependent transcriptional addiction in triple-negative breast cancer. Cell 163 174–186. [PubMed: 26406377]

Wilhelm S, Carter C, Lynch M, Lowinger T, Dumas J, Smith RA, Schwartz B, Simantov R & Kelley S 2006 Discovery and development of sorafenib: a multikinase inhibitor for treating cancer. Nature Reviews Drug Discovery 5 835–844. [PubMed: 17016424]

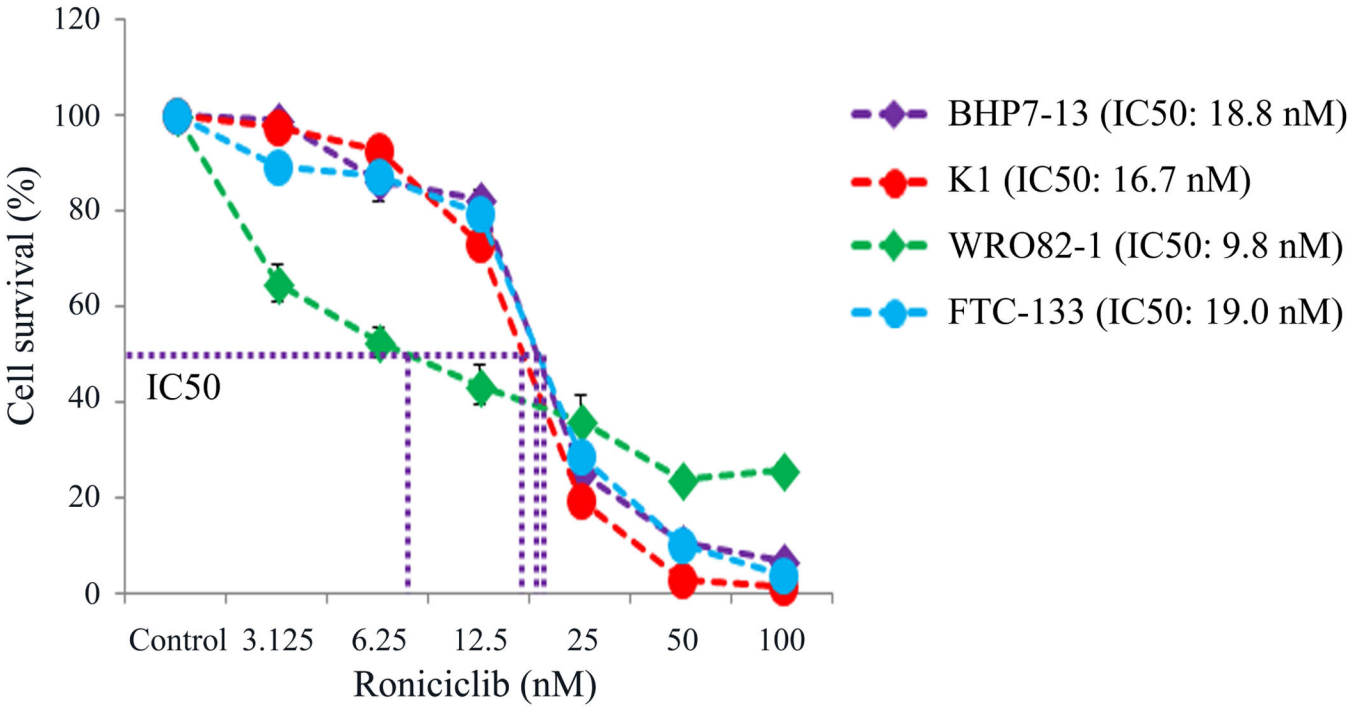

Figure 1.

Roniciclib induces cytotoxicity in well-differentiated thyroid cancer cells. Cytotoxicity was evaluated in cells treated with a series of six two-fold dilutions of roniciclib starting from 100 nmol/L. Dose-response curves were obtained on day 4 using LDH assays. The median-effect dose (IC50) of roniciclib on day 4 was calculated for each cell line using CompuSyn software.

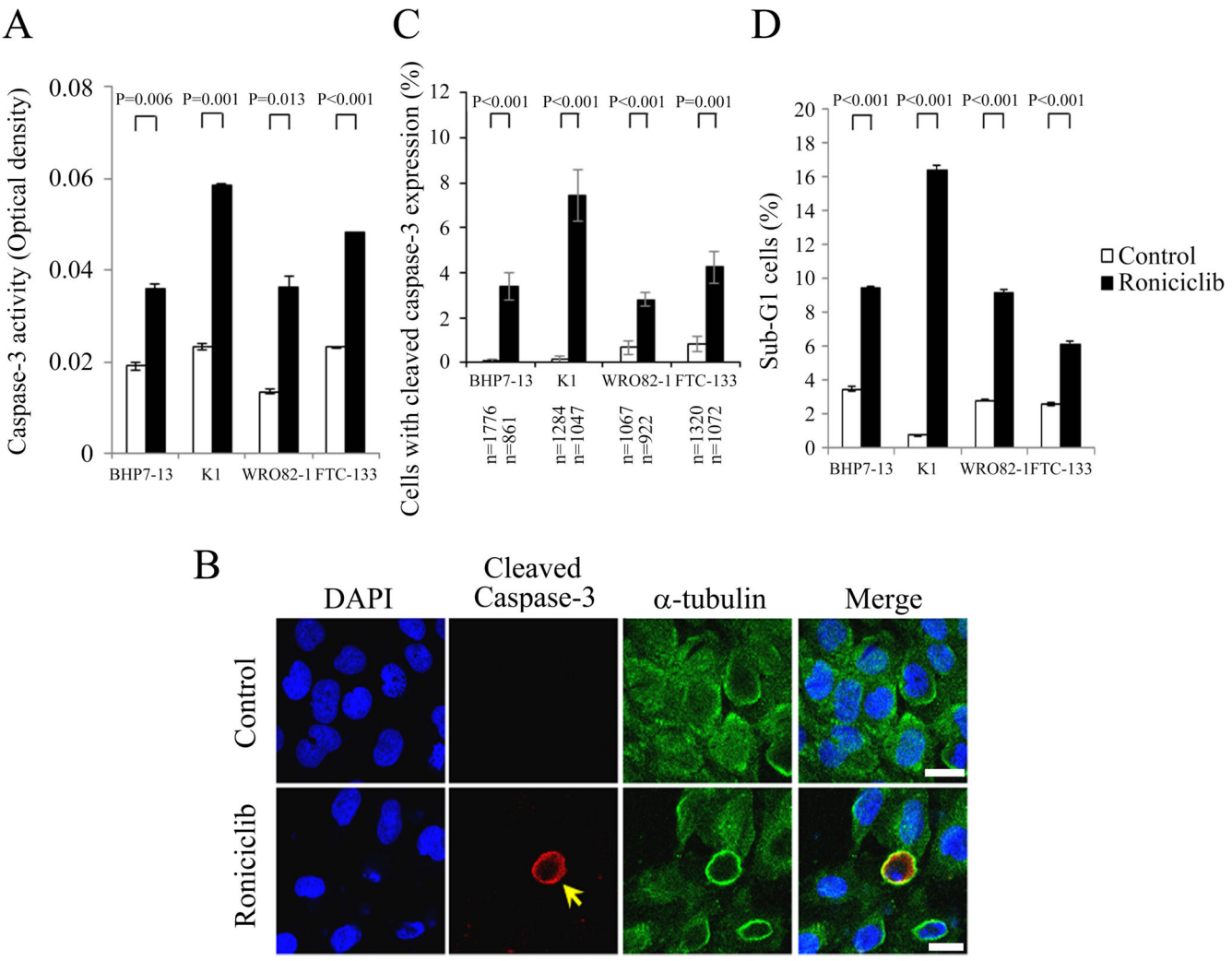

Figure 2.

Roniciclib stimulates caspase-3 activity and induces apoptosis in well-differentiated thyroid cancer cells. (A) Caspase-3 activity was evaluated using a fluorometric assay kit in BHP7–13, K1, WRO82–1 and FTC-133 cells treated with roniciclib (25 nmol/L) or vehicle for 24 h. (B) BHP7–13 cells were treated with roniciclib (25 nmol/L) or placebo for 24 h and stained with DAPI (blue) and fluorescent antibodies against cleaved caspase-3 (red) and α-tubulin (green). A cell with cleaved caspase-3 expression is shown (arrow). (C) The percentages of cells with cleaved caspase-3 expression were assessed after treatment with placebo or roniciclib (25 nmol/L) for 24 h. Cells were stained with fluorescent antibodies against cleaved caspase-3, and its expression was evaluated using immunofluorescence confocal microscopy. A minimum of 861 cells from at least 12 different fields was counted for each condition. Roniciclib significantly increased the proportion of BHP7–13, K1, WRO82–1 and FTC-133 cells with cleaved caspase-3 expression. (D) Sub-G1 apoptotic cells were detected by measuring the DNA content using flow cytometry in cells treated with roniciclib (25 nmol/L) or vehicle for 24 h. Roniciclib increased the proportion of sub-G1 cells in four well-differentiated thyroid cancer cell lines. Scale bar, 20 μm.

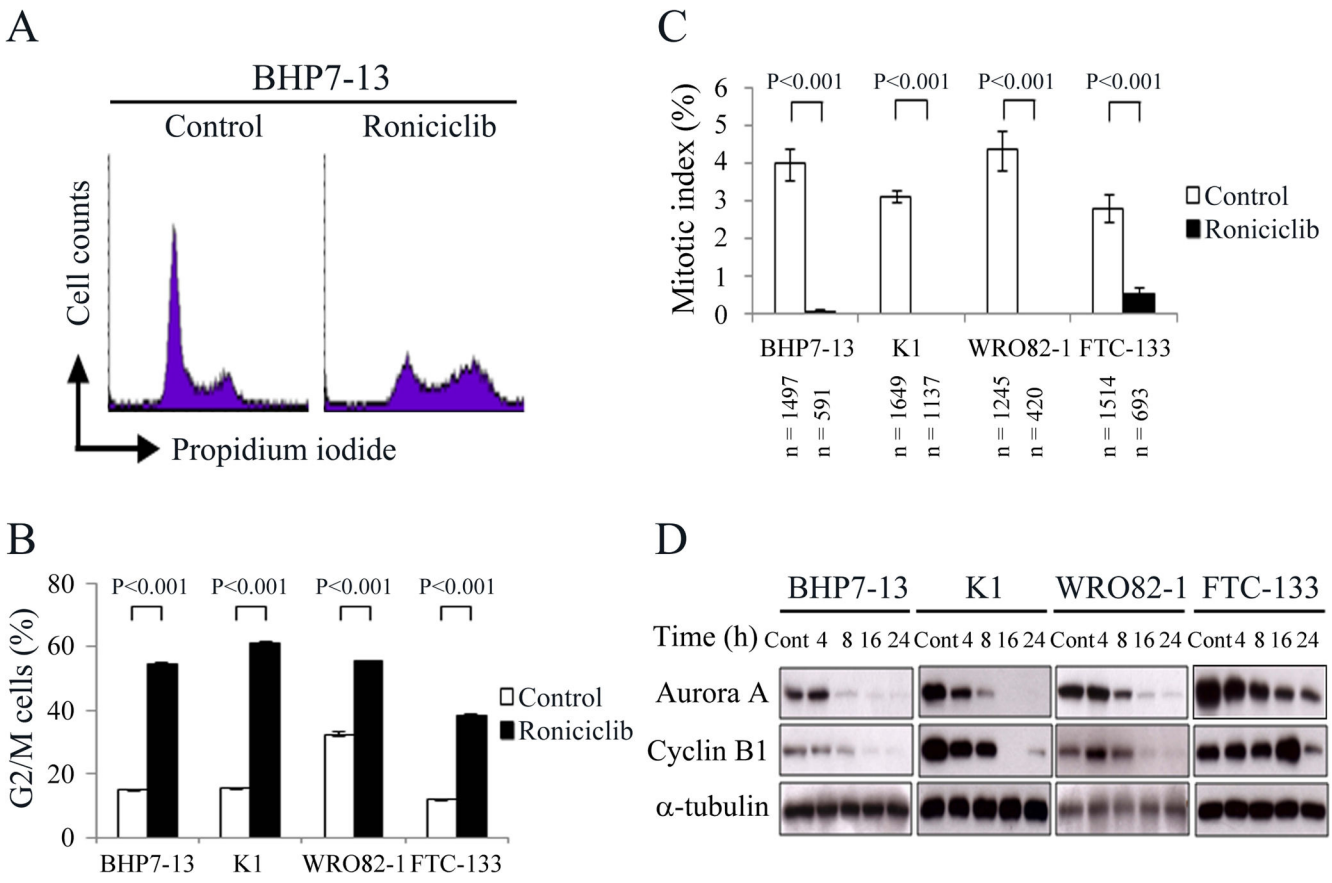

Figure 3.

Roniciclib decreases the protein levels of aurora A and cyclin B1 and induces G2/M phase accumulation in well-differentiated thyroid cancer cells. (A) Cell cycle distribution was analyzed by evaluating the DNA content in BHP7–13 cells treated with placebo or roniciclib (25 nmol/L) for 24 h using flow cytometry. (B) Statistical analyses revealed that roniciclib treatment (25 nmol/L) significantly arrested BHP7–13, K1, WRO82–1 and FTC-133 cells in the G2/M phase at 24 h. (C) The proportion of well-differentiated thyroid cancer cells in mitosis was assessed after treatment with roniciclib (25 nmol/L) or placebo for 24 h. Cells were stained with DAPI, and chromosome characteristics were evaluated using immunofluorescence confocal microscopy. The mitotic index was assessed with a minimum of 420 cells counted from at least 10 different fields for each condition. Roniciclib significantly decreased the proportion of BHP7–13, K1, WRO82–1 and FTC-133 cells in mitosis. (D) The expression of aurora A and cyclin B1 was evaluated by Western blotting in BHP7–13, K1, WRO82–1 and FTC-133 cells treated with roniciclib (25 nmol/L) or placebo for the indicated periods.

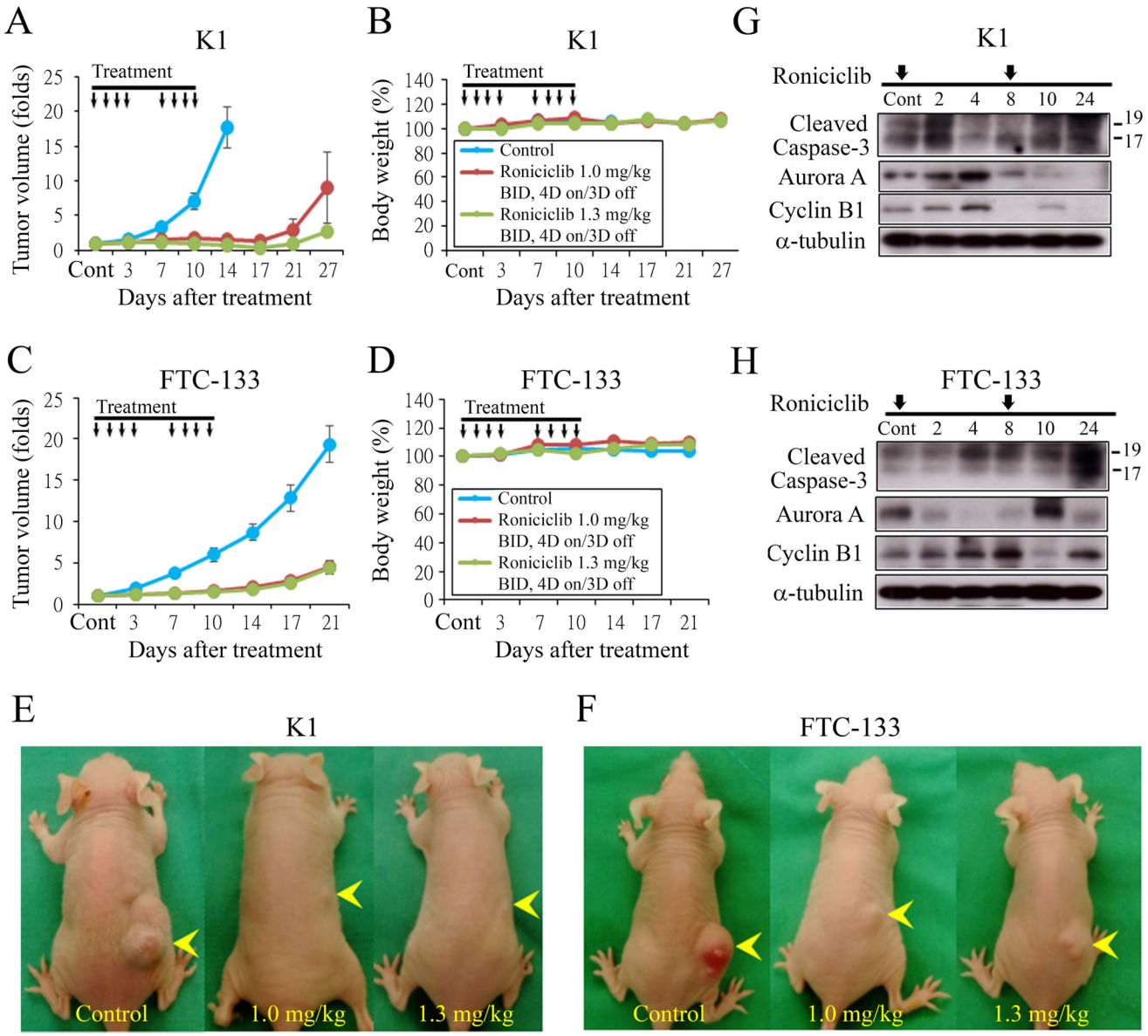

Figure 4.

Roniciclib inhibits subcutaneous xenograft growth of two well-differentiated thyroid cancer models. (A) The therapeutic efficacy of roniciclib for papillary thyroid cancer was evaluated in mice bearing K1 flank tumors. Serial oral gavage of low-dose (1.0 mg/kg) and high-dose (1.3 mg/kg) roniciclib significantly repressed K1 tumor growth by day 3 when compared with control mice, and the effect persisted through day 14. (B) Serial treatment of low-dose (1.0 mg/kg) and high-dose (1.3 mg/kg) roniciclib did not significantly decrease body weight when compared with control mice. (C) The therapeutic efficacy of roniciclib for follicular thyroid cancer was evaluated in mice bearing FTC-133 flank tumors. Serial oral gavage of low-dose (1.0 mg/kg) and high-dose (1.3 mg/kg) roniciclib significantly repressed FTC-133 tumor growth by day 3 when compared with control mice, and the effect persisted through day 21. (D) Serial treatment of high-dose roniciclib (1.3 mg/kg) slightly, but significantly induced body weight loss on day 10 when compared with control mice. This effect was not

observed in mice treated with low-dose (1.0 mg/kg) roniciclib. K1 (E) and FTC-133 (F) xenograft tumors (arrowhead) were photographed on day 15. The molecular effects of roniciclib (1.3 mg/kg) treatment were evaluated in K1 (G) and FTC-133 tumors (H) using Western blot analysis. Arrow, roniciclib or placebo treatment.

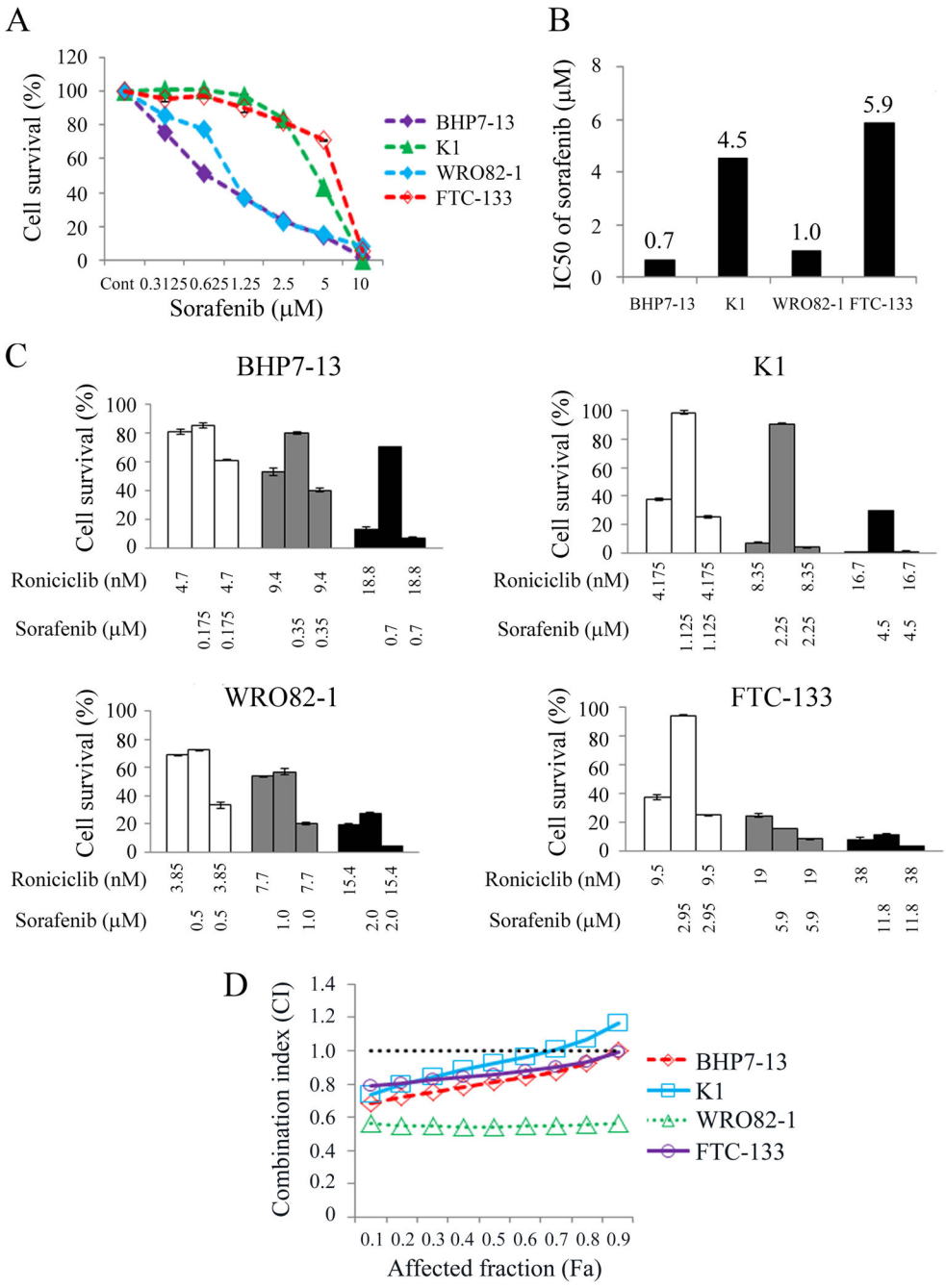

Figure 5.

Combination therapy of roniciclib and sorafenib in well-differentiated thyroid cancer cells. (A) Cytotoxicity was evaluated in BHP7–13, K1, WRO82–1 and FTC-133 cells treated with a series of six two-fold dilutions of sorafenib starting at 10 μmol/L. Dose-response curves were obtained on day 4 using LDH assays. (B) The median-effect dose (IC50) of sorafenib on day 4 was calculated for each cell line using CompuSyn software. (C) The cytotoxic effects of roniciclib and sorafenib alone and in combination after a 4-day treatment in BHP7–13, K1, WRO82–1 and FTC-133 cells were evaluated using LDH assays. (D) The combination index (CI) of roniciclib and sorafenib was calculated using CompuSyn

software. The combination therapy of roniciclib and sorafenib had synergistic effects in WRO82–1 and FTC-133 cells, synergistic to additive effects in BHP7–13 cells and synergistic to antagonistic effects in K1 cells. Synergistic effects appeared when the affected fractions of BHP7–13 and K1 cells was lower (affected fraction < 0.9 and < 0.7, respectively). The horizontal line at CI = 1 was drawn for discrimination of synergism (CI < 1) and antagonism (CI > 1).

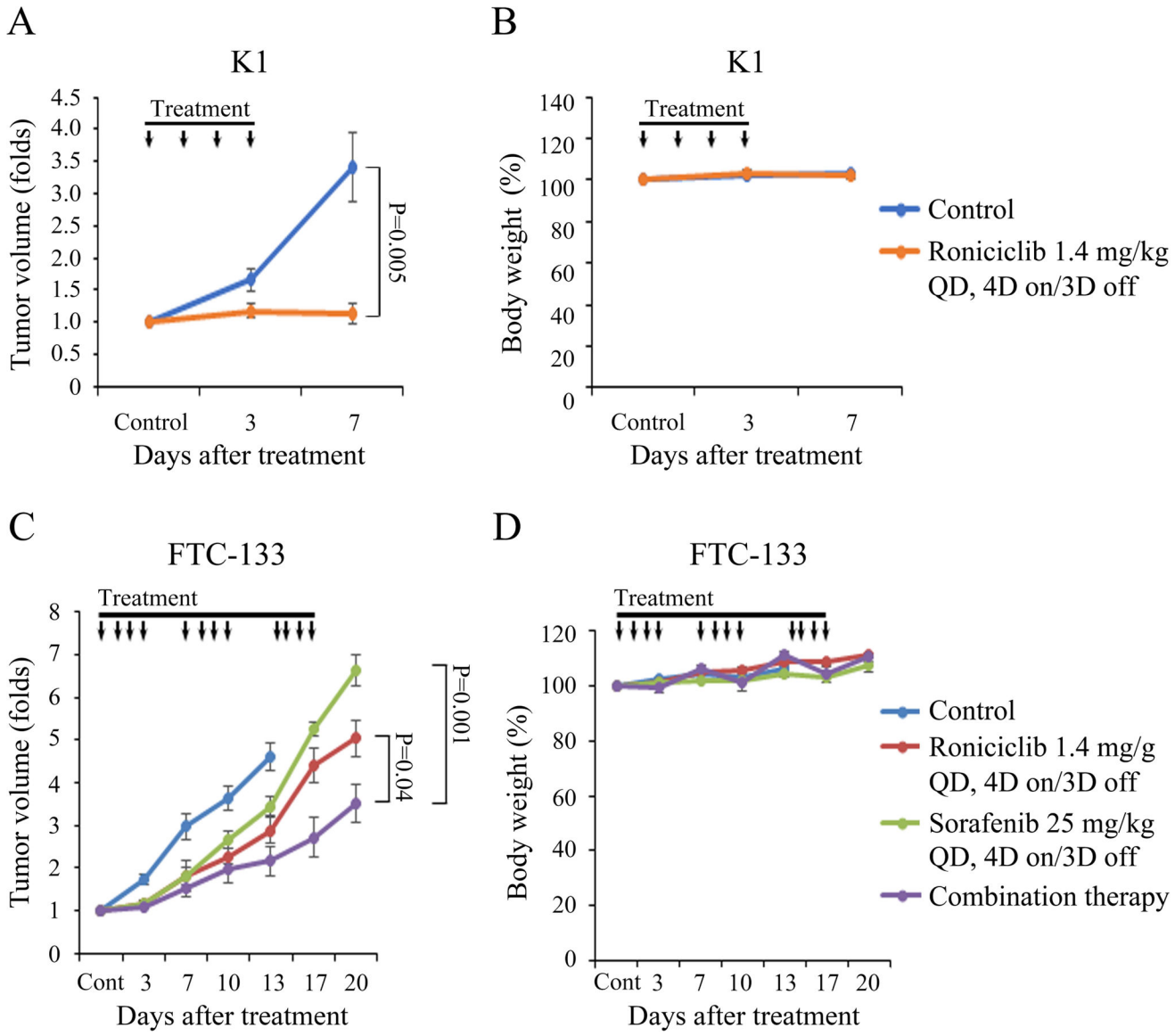

Figure 6.

Daily therapy of roniciclib and sorafenib in murine well-differentiated thyroid cancer xenograft tumor models. (A) Daily treatment of roniciclib (1.4 mg/kg) for 4 days significantly inhibited subcutaneous xenograft growth of K1 tumors compared with control mice on day 7. (B) Serial daily administration of roniciclib did not result in significant changes in body weight during the study period. (C) After FTC-133 flank tumors were established in nude mice, they were treated with oral gavage of placebo, roniciclib (1.4 mg/kg), sorafenib (25 mg/kg) or combination therapy once a day for three cycles of 4-day on and 3-day off therapy. Compared with control therapy, roniciclib, sorafenib and combination treatment all significantly inhibited tumor growth by day 3, and the inhibitory effects persisted through day 13. Combination therapy significantly retarded xenograft growth when compared with either single modality treatment on days 17 and 20. (D) No significant decreases in body weight were attributable to placebo, roniciclib, sorafenib or combination

therapy compared with the baseline weight. Arrow, placebo, roniciclib, sorafenib and combination treatment.